

The Unusual Southern Hemisphere Stratosphere Winter of 2002

PAUL A. NEWMAN

NASA Goddard Space Flight Center, Greenbelt, Maryland

ERIC R. NASH

Science Systems and Applications, Inc., Landover, Maryland

(Manuscript received 15 May 2003, in final form 16 January 2004)

ABSTRACT

The Southern Hemisphere (SH) stratospheric winter of 2002 was the most unusual winter yet observed in the SH climate record. Temperatures near the edge of the Antarctic polar vortex were considerably warmer than normal over the entire course of the winter. The polar night jet was considerably weaker than normal and was displaced more poleward than has been observed in previous winters. These record high temperatures and weak jet resulted from a series of wave events that took place over the course of the winter. The propagation of these wave events from the troposphere is diagnosed from time series of Eliassen–Palm flux vectors and autoregression time series. Strong levels of planetary waves were observed in the midlatitude lower troposphere. The combinations of strong tropospheric waves with a low index of refraction at the tropopause resulted in the large stratospheric wave forcing. The wave events tended to occur irregularly over the course of the winter, and the cumulative effect of these waves was to precondition the polar night jet for the extremely large wave event of 22 September. This large wave event resulted in the first ever observed major stratospheric warming in the SH and split the Antarctic ozone hole. The combined effect of all of the 2002 winter wave events resulted in the smallest ozone hole observed since 1988. The sequence of stratospheric wave events was also found to be strongly associated with unusually strong levels of wave 1 in the SH tropospheric subtropics.

1. Introduction

During the fall of 2002, the Antarctic ozone hole was unusually disturbed (Stolarski et al. 2005). First, the ozone hole was considerably smaller than has been observed during early September. Second, the ozone hole split into two parts on 22 September. This unusual behavior was not a result of changing chlorine and bromine levels, since stratospheric halogen levels have not significantly decreased over the last few years (Montzka et al. 2003), but was because of the stratospheric temperature and dynamics that occurred over the winter. There are two necessary conditions for causing the Antarctic ozone hole: high levels of halogens (specifically chlorine and bromine; see WMO 1995) and temperatures cold enough to form polar stratospheric clouds (PSCs).

The impact of dynamics on the Antarctic ozone hole has always been considered to be of secondary importance because temperatures are always cold enough to

form extensive PSCs, and the Southern Hemisphere (SH) has small interannual variability during winter (Randel 1992). It has long been recognized that Antarctic September temperatures are extremely cold (i.e., temperatures <193 K, the approximate formation temperature for PSCs). For example, Court (1942) noted the very cold winter conditions from balloon observations during September 1940 at Little America (78°S) and remarked “... since in general, soundings ended prematurely as soon as they reached -80°C level, apparently the limit of balloon elasticity.” In contrast, Arctic temperatures are both warmer and more variable. This variability occasionally results in large Arctic ozone losses (e.g., 1997) or virtually no ozone loss at all (e.g., 1999; Rex et al. 2002).

This unusual winter challenges our understanding of the SH stratosphere, namely, that the SH stratosphere is typically very cold because wave forcing is weak. The occurrence of such a winter could be driven by internal processes or possibly climate change effects. Our ability to predict future Antarctic ozone levels is constrained by our understanding of the dynamics and climate forcings that control the stratospheric temperatures in the Antarctic stratosphere. Hence it is extremely important to understand why the winter of 2002 was so unusual.

Corresponding author address: Dr. Paul A. Newman, NASA Goddard Space Flight Center, Mail Code 916, Greenbelt, MD 20771.
E-mail: newman@code916.gsfc.nasa.gov

Therefore, it is necessary to 1) understand the morphology of this winter's evolution in contrast to climatology, 2) describe the sequence of wave events over the course of the winter, and 3) understand the formation and propagation of these events.

This paper will describe the evolution of the 2002 SH winter. First, the unusual stratospheric winter developed from a sequence of large amplitude wave events that spanned the entire winter. These waves varied in strength and duration, with the largest and most spectacular being the major warming of 22 September that split the ozone hole into two pieces (Hoppel et al. 2003). Second, each wave event acted to warm the region near the polar night jet ($\sim 65^{\circ}\text{S}$); that is, the winter was characterized by a series of minor warmings and a single major warming. The total wave energy propagating into the stratosphere quantitatively explains the much warmer than normal temperatures during September. Third, the polar vortex broke down earlier than normal. The typical warming of the SH has a regular downward progression that usually begins in July in the upper stratosphere and ends in late November in the lower stratosphere. In 2002, this same downward progression of warming also occurred but at an accelerated rate because of the greater number of wave events over the course of the winter. Fourth, eddy variance in the troposphere was large, but did not exhibit a systematic pattern over the winter. Fifth, the wave events observed over the course of the winter are traceable to the troposphere. Finally, the wave-1 pattern was clearly anomalous during the winter of 2002 from the Tropics to the high latitudes.

2. Data

The National Centers for Environmental Prediction–National Center for Atmospheric Research reanalysis (NRR) data are used as the basis for this work. These analyses are restricted to data after 1978 because of the poorer quality of the NRR data in the stratosphere prior to the inclusion of satellite observations in 1979 (Mo et al. 1995; Kanamitsu et al. 1997; Santer et al. 1999; Marshall 2002). In addition, certain quantities calculated, such as the heat flux, exhibit considerable uncertainty in both hemispheres (Newman and Nash 2000; Randel et al. 2002). Northern Hemisphere (NH) flux values from a variety of analyses show differences of $\pm 15\%$ (Newman and Nash 2000), while a comparison of the SH heat flux between the NRR and European Centre for Medium-Range Weather Forecasts analyses by Randel et al. (2002) shows large differences. Nevertheless, the differences between the year 2002 and the climatology are large compared to the overall analysis errors.

3. Results

Temperatures near the jet axis were higher than normal in the polar stratosphere during the entire winter.

The black line in Fig. 1c displays the zonal-mean daily temperature at 65°S and 50 hPa during the 2002 winter, while the white line shows the climatological average. Up to the middle of May, temperatures at 65°S (near the core of the vortex) were near normal. There was a slight increase in the middle of May, followed by a relaxation back to normal temperatures until the middle of June. By late June, temperatures were well above normal and were regularly higher than any values observed at a comparable time over the last 24 years. In late September, the temperature dramatically increased to values that were 15 K warmer than average.

In contrast to the temperatures near the jet axis, temperatures in the core of the vortex (near the South Pole) were only slightly higher than normal over most of the winter. Figure 1b displays the minimum daily temperature observed between 50° and 90°S at 50 hPa during the 2002 winter. Again, the white line shows the average minimum temperature. Only in late September does the temperature jump to a value that is higher than climatology.

Temperatures at higher altitudes inside the vortex were slightly colder than average during the winter. Figure 1a displays the minimum daily temperature ob-

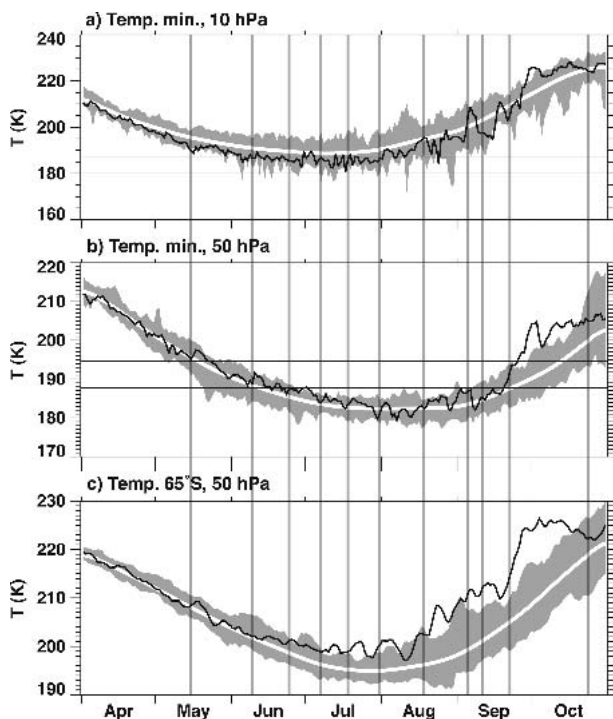


FIG. 1. Daily min temperature averaged over 50° – 90°S at (a) 10 and (b) 50 hPa. (c) Daily zonal-mean temperature at 65°S and 50 hPa. The black line in each panel shows the 2002 temperature. The white line displays the 23-yr average (1979–2001) and is smoothed with a 15-day boxcar. The gray shading indicates the range of values observed between 1979 and 2001. The vertical gray lines passing through all panels indicate the days of max eddy heat flux at 100 hPa.

served between 50° and 90°S at 10 hPa during the 2002 winter. At these higher altitudes, the 2002 temperatures were generally below the climatological daily average (white line). The exceptions occur in early September and late September through October. These colder than normal temperatures at higher altitudes suggest that PSCs may have been forming at altitudes much higher than normal during the 2002 winter, with the consequent conversion of HCl and ClONO₂ into reactive forms.

The vertical structure of these warmer than normal temperatures near the edge of the vortex are displayed in Fig. 2a. This figure shows the 2002 SH zonal-mean temperature departures from the 1979–2001 mean near the core of the polar night jet (55°–75°S). During April to early May, temperatures are near normal. A minor

warming occurs in the middle of May. By early June, temperatures begin to steadily increase with respect to the climatological average. By early July, these temperatures have increased to extremely high values, with further increases culminating in a major stratospheric warming on 22 September. A major warming is defined by a reversal of the zonal-mean temperature gradient between 50° and 80°S, combined with a reversal of the very strong 60°S zonal wind at 10 hPa to easterlies. The temperature differences from climatology became increasingly warmer over the course of the winter as a result of stepwise warming with some cooling after each warming. The warming appears to descend over the course of the winter. For example, the May and June warmings peak near or above 10 hPa and only extend down to about 100 hPa, the August temperature

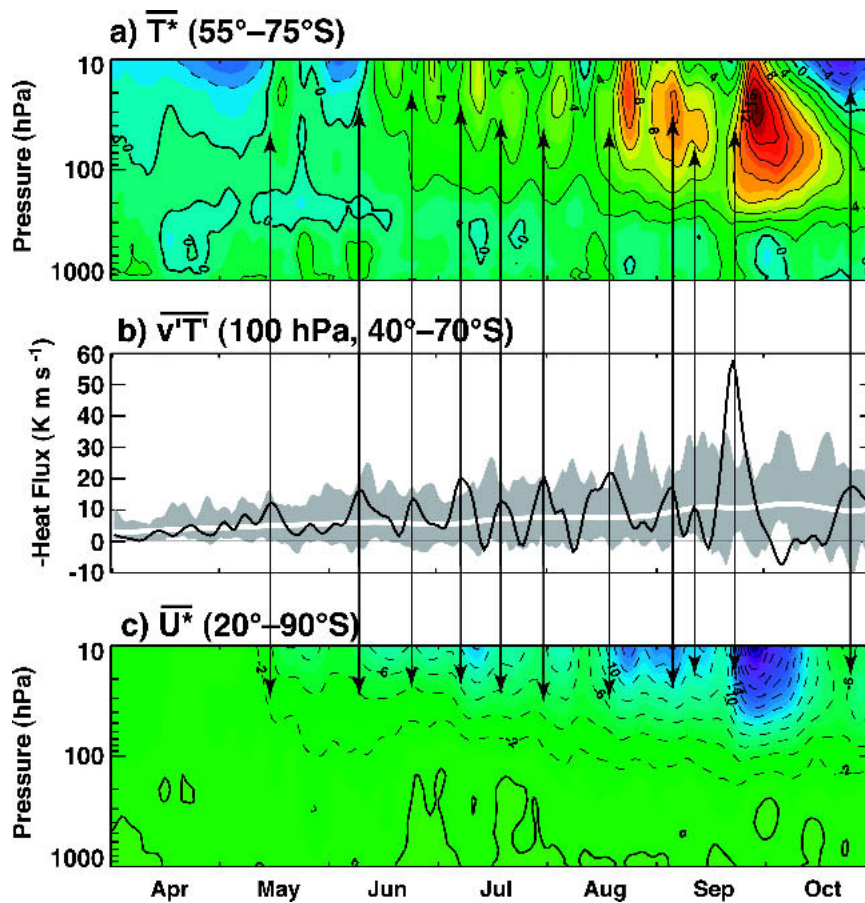


FIG. 2. (a) Daily temperature departures ($\overline{T^*}$) from the 1979–2001 mean for 1 Apr to 31 Oct 2002, averaged for 55°–75°S at 50 hPa. Contour intervals are 2 K and negative contours are dashed. (b) Daily eddy heat flux ($\overline{v'T}$) at 100 hPa, averaged for 40°–70°S. Units are in K m s^{-1} . The black line shows the 2002 values, which have been smoothed with a 1–2–1 filter applied three times. The white line displays the 23-yr average (1979–2001) and is smoothed with a 15-day boxcar. The gray shading indicates the range of values (also 1–2–1 filtered) observed between 1979 and 2001. (c) Daily zonal-mean zonal wind ($\overline{U^*}$) departures from the 1979–2002 mean, averaged for 20°–90°S. Contour intervals are 2 m s^{-1} and negative contours are dashed. The vertical lines passing through all panels indicate the days of max eddy heat flux at 100 hPa. The primes denote the departures from the zonal mean, the overbars denote the zonal mean, and the asterisks denote the departures from the 1979–2001 mean.

anomalies peak below 10 hPa and extend below 100 hPa, and the September major warming peaks near 30 hPa and extends below 300 hPa.

The warming of the polar vortex collar region is directly controlled by the planetary waves that propagate upward from the troposphere into the stratosphere (Hartmann et al. 1984; Shiotani and Gille 1987). The black line in Fig. 2b is a 2002 time series of midlatitude eddy heat flux at 100 hPa for waves 1–3. As discussed in Andrews et al. (1987), the heat flux represents the vertical flux of wave energy. After each of these wave events, the stratosphere has been warmed by a few degrees. Over the course of May–October, there are 11 significant wave events (Table 1). Vertical lines are superimposed between the panels of Fig. 2 to show the connection between the wave events and the warmings. The wave events are irregularly spaced with about a 1–3 week periodicity.

The 2002 wave events are large compared to the climatological average (white line). The gray shading shows the range of these daily values over 1979–2001. The wave events of 8 July, 18 August, and 22 September are all records. The 22 September event is unprecedented. Further, the level of the eddy heat flux is higher than the climatological average for a considerable fraction of the winter.

The waves not only impact temperature, but also the zonal wind. Figure 2c displays the zonal-mean zonal wind difference between 2002 and a 1979–2001 average over 20°–90°S. This figure effectively represents the deviation of the average polar night jet strength from climatology. Each wave noted in Fig. 2b impacts the strength of the jet in Fig. 2c, with the 22 September wave completely reversing the westerlies to weak easterlies. Combined with the temperature increase shown in Fig. 2a and Fig. 1, it is clear that this event was the first major stratospheric warming yet observed in the SH. However, it is important to recognize that the flow was first disturbed by the 15 May event and was highly disturbed by the middle of August.

The wave events over the course of the winter cumulatively acted to warm the polar lower stratosphere. Furthermore, this warming is fairly consistent with previous winters. Figure 3a displays the late-September polar temperature at 50 hPa plotted against the average midlatitude heat flux for a 53-day period, consisting of 45 days prior to the first day of the temperature period and overlapping into the temperature period by 8 days. The two quantities are highly correlated. In essence, the accumulating effect of the wave flux into the stratosphere over August–September is to warm the polar region [see Newman et al. (2001) for a discussion of comparable effects in the Arctic]. During 2002, the late-September temperatures were significantly warmer than any previous winter because of the unusual strength and duration of the wave events. Most of the impact of these wave events on temperatures tends to occur near the edge of the vortex (near the jet axis, ~55°–75°S). While the wave events are apparent in the core of the vortex (see Fig. 1a), the effect there is smaller than at the edge.

The cumulative effect of the waves also impacted the temperatures prior to the major warming shown in Fig. 2a. Figure 3b displays the early-September polar temperature at 50 hPa plotted against the average midlatitude heat flux for a 53-day period prior to this temperature period. Again, note the excellent correlation. Early September 2002 had the highest temperature with the highest midwinter heat flux. While the 1986 heat flux was comparable to 2002, the flux in early winter of 1986 was smaller than in 2002. The major difference between 1986 and 2002 was the late-September major warming in 2002. By shifting the time average by 15 days, the average heat flux in 2002 changes by about 5 K m s⁻¹, an indicator of the magnitude of the late-September 2002 wave event.

The spatial pattern of warm temperatures covers a considerable region of the SH by late August. However, as mentioned previously, the warmer than normal temperatures were predominantly in the region near

TABLE 1. Significant 2002 wave events as indicated by the 100-hPa eddy heat flux averaged over 40°–70°S. Dates listed are when the peak in wave-1–3 eddy heat flux is maximum. Number of days in an event is determined by when the sign of the first derivative changes on either side of the peak. Total, W1, W2, and W3 represent wave-1–3, -1, -2, and -3 amplitude of eddy heat flux (K m s⁻¹); WN is the dominant wavenumber(s) for the event; and ΔT is the difference in 50-hPa temperature departures from the 1979–2001 daily means, averaged over 60°–90°S, between criteria used for the number of days (K). Bold values represent the maximum values between W1, W2, and W3 on a particular day.

Date	Number of days	Total	W1	W2	W3	WN	ΔT
15 May	5	-13.86	-7.31	-4.31	-2.24	1,2	2.0
9 Jun	4	-19.72	-2.80	-14.48	-2.44	2	1.2
24 Jun	4	-16.75	-4.29	-5.98	-6.47	1,2,3	1.9
8 Jul	7	-20.01	-12.88	-5.16	-1.97	1	1.8
19 Jul	7	-14.69	1.46	-8.96	-7.19	2,3	2.4
31 Jul	6	-26.02	-5.95	-18.29	-1.79	2	1.5
18 Aug	6	-25.41	-16.43	-6.10	-2.87	1	9.1
5 Sep	5	-24.64	-1.35	-22.67	-0.63	2	1.7
11 Sep	3	-15.41	-0.66	-6.43	-8.31	2,3	0.6
22 Sep	4	-70.43	-25.30	-28.31	-16.82	1,2,3	4.9
26 Oct	8	-18.01	-18.18	0.69	-0.51	1	-4.3

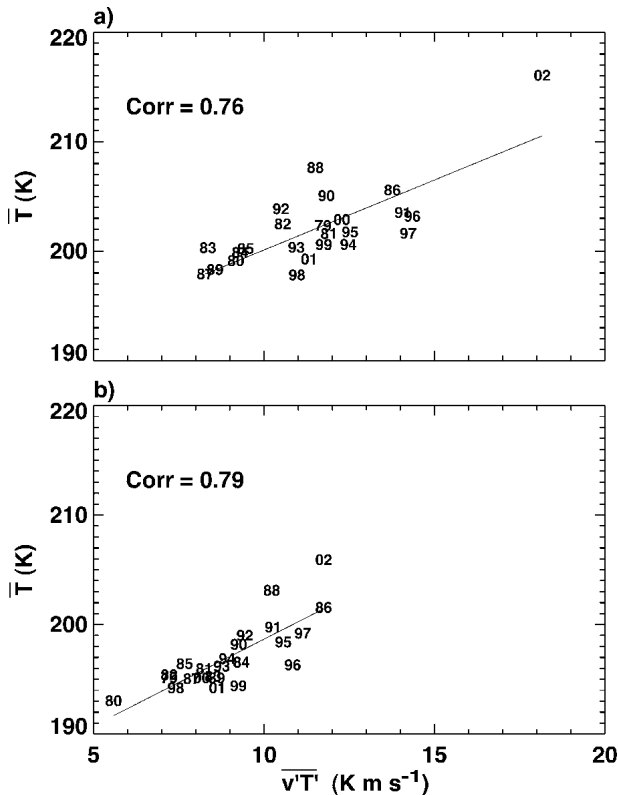


FIG. 3. Temperature (\bar{T}) at 50 hPa and averaged for 60°–90°S plotted against eddy heat flux ($\overline{v'T'}$) at 100 hPa and averaged for 40°–70°S. (a) Temperature averaged for 16–30 Sep and eddy heat flux averaged for 2 Aug–23 Sep. (b) Temperature averaged for 1–15 Sep and eddy heat flux averaged for 18 Jul to 8 Sep. The solid line is the least squares regression fit and the correlations are shown. Each year is indicated by the last two digits. The primes denote the departures from the zonal mean and the overbars denote the zonal mean.

the jet core. Figure 4a shows temperature differences between July 2002 and a 1979–2001 climatology. The climatology is superimposed on the figure as white lines. Zonal-mean temperatures are much warmer than normal near the climatological jet core and vortex edge. In the vortex core near the pole, temperatures are only 1–2 K warmer than climatology in the lower stratosphere, in agreement with the minimum temperatures shown in Fig. 1b. In addition, the temperatures at higher altitude (above 20 hPa) inside the vortex were colder than normal, in agreement with the minimum temperatures shown in Fig. 1a.

The zonal-mean zonal wind was also very disturbed during July 2002, prior to the 22 September major warming. Figure 4b displays zonal-mean zonal wind differences between July 2002 and climatology. The jet core was closer to the pole during 2002, and so the polar vortex was somewhat smaller. The zero-wind line in the lower to middle stratosphere was approximately 6°–10° closer to the pole in 2002 than the climatological average. The series of wave events shown in Fig. 2b decel-

erated the jet as shown in Fig. 2c, leading to the smaller and weaker vortex by July and into September. Furthermore, the shift of the jet also shifted the maximum of the index of refraction toward the South Pole.

The quasi-biennial oscillation (QBO) was in the westerly phase in 2002, as is apparent from the positive anomaly near the equator at 20–30 hPa in Fig. 4b. In addition, winds in the upper-stratospheric Tropics were in the easterly phase (not shown on Fig. 4b).

The upper-tropospheric subtropical jet position was also anomalous during the winter of 2002. This jet was shifted southward by 1.8° of latitude on average for the period of 1 June to 1 September. The position of the jet at 30.3°S was the most southerly displacement seen in the 24-yr period (1979–2002). The wind speed was stronger than average but was not a record high. Note

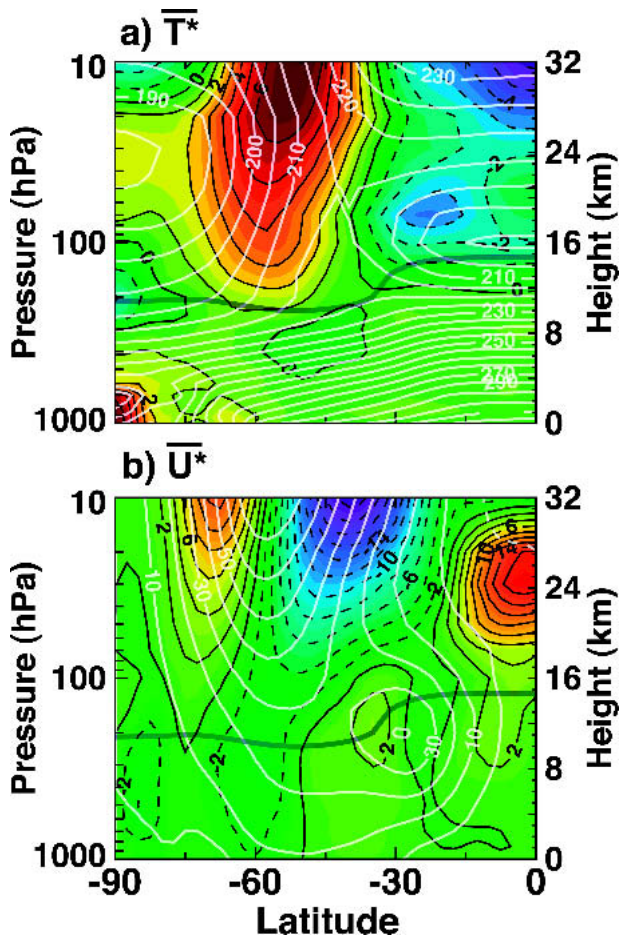


FIG. 4. (a) Jul zonal-mean temperature departures (\bar{T}^*) from the long-term mean (1979–2001). Contour intervals are 1 K. The white contours are the long-term mean field, with intervals of 5 K. (b) Jul zonal-mean zonal wind departures (\bar{U}^*) from the long-term mean (1979–2001). Contour intervals are 2 m s⁻¹. The white contours show the long-term mean field, with intervals of 10 m s⁻¹. Negative contours are dashed in both panels. The overbars denote the zonal mean and the asterisks denote the departures from the 1979–2001 mean.

the 2 m s^{-1} positive anomaly in Fig. 4b that is immediately to the south of the core of the subtropical jet.

The Eliassen–Palm (EP) flux is an extremely useful diagnostic for evaluating the propagation of waves in the stratosphere. Using small amplitude theory, it can be shown that the EP flux vector $\mathbf{F} = (0, F^{(\phi)}, F^{(z)})$ points in the direction of the wave's group velocity (Andrews et al. 1987). The EP flux is related to the eddy heat and momentum fluxes by

$$F^{(\phi)} = \rho_0 a \cos\phi (\overline{u_z v' \theta' / \theta_z} - \overline{v' u'}) \quad (1)$$

$$F^{(z)} = \rho_0 a \cos\phi \{ [f - (a \cos\phi)^{-1} (\overline{u \cos\phi})_{,\phi}] \overline{v' \theta' / \theta_z} - \overline{w' u'} \}, \quad (2)$$

where ρ_0 is the density, a is the earth's mean radius, ϕ is the latitude, z is log-pressure height, u, v, w are the zonal, meridional, and vertical wind components, θ is the potential temperature, f is the Coriolis parameter, $\overline{v' \theta'}$ is the eddy potential temperature flux (scaled by a pressure function to obtain the heat flux), $\overline{v' u'}$ is the horizontal eddy momentum flux; the overbar denotes zonal-mean quantities, the prime indicates departures from the zonal mean, and subscripts indicate derivatives with respect to the variable indicated. The term involving the vertical eddy momentum flux $\overline{w' u'}$ has been ignored in our calculations.

The EP flux is shown as a function of altitude and time (Fig. 5a), and latitude and time for 200 (Fig. 5b) and 700 hPa (Fig. 5c). Poleward-tilting EP flux vectors are shown in red, while equatorward-tilting vectors are in black. These EP flux vectors are calculated from waves 1 to 3 (i.e., planetary scales). The vertical lines indicate the major wave events diagnosed from the 100-hPa heat flux, as shown in Fig. 2b. In the 150–200-hPa region of the stratosphere, the waves on average propagate upward and equatorward (see Fig. 5a). The large exception to this case occurs in September during the major warming wave event. A close inspection of Fig. 5a shows that the waves are strongly propagating toward the pole over a broad altitude region extending into the middle stratosphere. This convergence into the polar cap produces the sudden warming by rapidly decelerating the mean wind and warming the polar region. Further examination of the figure shows that the poleward propagation of this 22 September wave extends well into the troposphere. As discussed previously with Fig. 4b, the stratospheric polar night jet axis and the maxima of the index of refraction were tilted more poleward by early September. This poleward tilt resulted from the wave events over the course of the winter, preconditioning the flow for the major warming of 22 September.

As noted above, the wave event of 22 September propagated into the polar region over a very large vertical depth. Figure 5b displays the EP flux vectors on the 200-hPa surface. In Figs. 5b and 5c, the vectors pointing toward the left are upward propagating, while

vectors pointing up are propagating equatorward. This figure shows that the upward propagation of waves in the upper troposphere occurs over a broad latitudinal extent (35° – 65° S). Furthermore, all of the wave events at 200 hPa show some poleward wave propagation. The EP flux at 700 hPa (Fig. 5c) also shows this strong upward flux.

The wave events shown in Fig. 2b did not exhibit a particularly coherent pattern over the course of the winter. For example, the 100-hPa eddy heat flux events shown in Fig. 2b are computed using only waves 1–3. Table 1 shows the dominant wave numbers associated with each warming. The wave events of 15 May, 8 July, 18 August, and 26 October were all dominated by strong wave-1 patterns, while the 9 June, 31 July, and 5 September events were dominated by wave-2 patterns. While the eddy heat flux is dominated by waves 1 and 2, wave 3 cannot be neglected.

The eddy variability of the streamfunction for the winter of 2002 is illustrated in Fig. 6. The streamfunction is derived from the nondivergent components of the NNR horizontal wind fields on pressure surfaces and is normalized by the radius of the earth. The streamfunction is analogous to the geopotential height, but has the advantage of directly showing planetary wave strength in the Tropics. Figure 6a displays the rms streamfunction wave amplitude as a function of altitude averaged over 40° – 70° S for waves 1–3. The rms amplitude has been normalized by the square root of the density to emphasize the tropospheric wave activity. Again, the vertical lines indicate the peak heat flux times at 100 hPa shown in Fig. 2b. The figure shows that the heat flux peaks are typically accompanied by coherent waves from the middle troposphere to 10 hPa, as also shown in Fig. 5a. Peak amplitudes in the upper troposphere typically precede the peak amplitudes at 10 hPa by a few days. In the stratosphere the wave amplitudes steadily strengthen over the course of the winter, reaching a maximum during the major warming in late September. The wave amplitudes are generally a maximum in the troposphere, with a minimum above the tropopause and a second maximum in the middle to upper stratosphere.

The planetary-scale eddy variability in the troposphere is concentrated in the 40° – 70° S region. Figure 6b shows the rms streamfunction wave amplitude for waves 1–3 at 200 hPa. In addition to the wave maxima in the 40° – 70° S region, there are wave activity maxima in the 10° – 30° S and 10° – 40° N regions. The wave activity peaks in the 10° – 30° S region appear about 3–10 days prior to the heat flux peaks (white vertical lines) in Fig. 6b. In addition, the wave activity peaks in the 10° – 40° N regions also appear to be correlated with the wave activity peaks in the 10° – 30° S region.

The wave event maxima vary in both strength and latitude location over the course of the winter. A Hovmöller diagram of the wave-1–3 eddy field is shown in Fig. 6c for a latitude of 60° S (gray horizontal line in

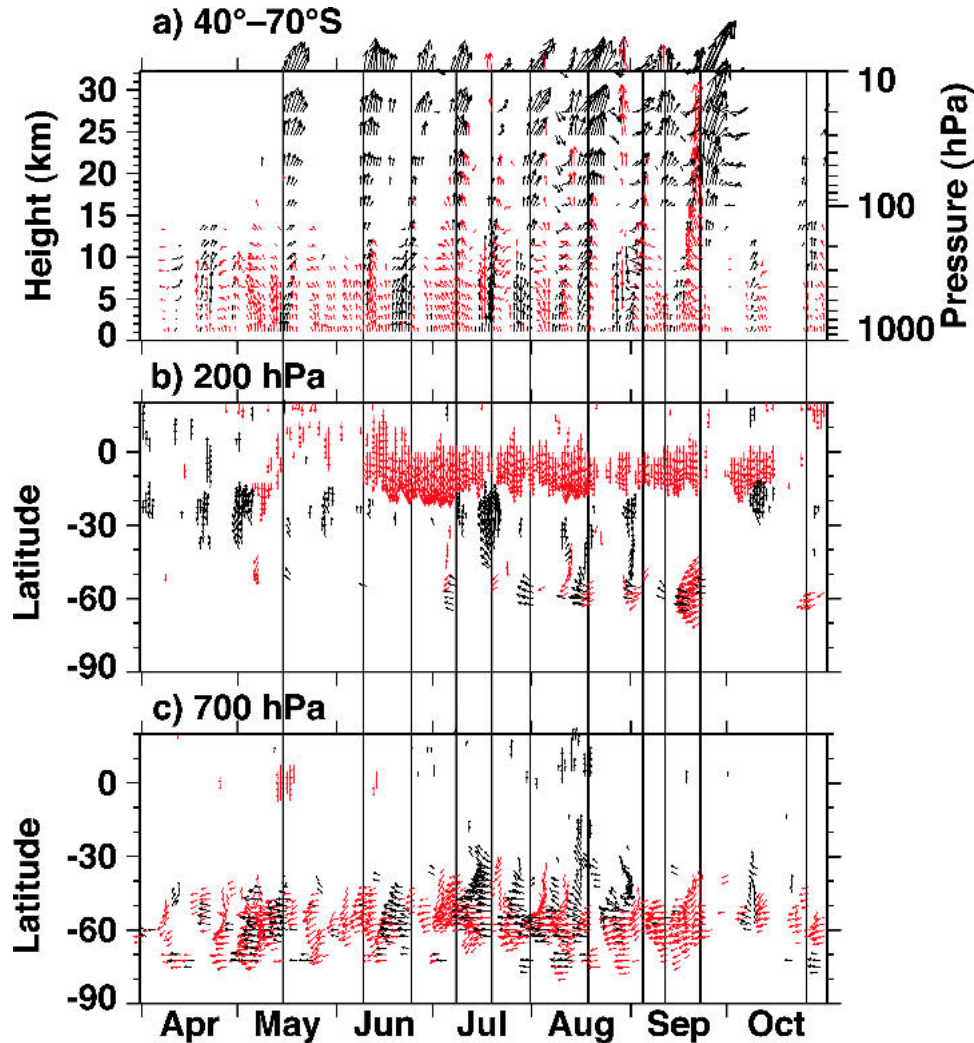


FIG. 5. (a) Daily EP flux vectors for waves 1–3 averaged from 40°–70°S. The vectors have been multiplied by the log of pressure to emphasize the lower altitude values. Vectors pointing up indicate vertical propagation, while vectors pointing to the right indicate equatorward propagation. Daily EP flux vectors at (b) 200 and (c) 700 hPa. In (b) and (c), vectors pointing upward indicate equatorward propagation, while vectors pointing to the left indicate upward propagation. In (a)–(c), EP flux vectors that make up less than 20% of the max vector over the whole field have not been plotted. Black arrows point equatorward and red arrows point poleward.

Fig. 6b). Note that the Hovmöller diagram is dominated by a wave-1 pattern, with the wave-1 peak centered at about 130°W (230°E), just west of the Antarctic Peninsula. The wave events primarily occur as episodic bursts of wave energy moving into the stratosphere with a wave event duration of 1–2 weeks.

Height and streamfunction field deviations from a 1979–2001 climatology in the upper troposphere for June–August (not shown) suggest a possible wave train that is forced in the Maritime Continent region of the western Pacific. Correlations of 100-hPa heat flux averages with the midwinter flow field suggest a relationship, namely, that strong anticyclonic flow to the west of the Antarctic Peninsula (approximately

60°S, 130°W) is associated with large-eddy activity in the tropical and subtropical troposphere.

We have investigated the vertical propagation of the planetary-scale waves using a cross-correlation analysis of the streamfunction. A cross-correlation analysis of the geopotential height field was used by Randel (1987) to investigate the propagation of planetary waves in the winters of 1983 and 1984. Figure 7 displays the coherence for wave 1 at 60°S and 100 hPa with wave 1 at other pressure values and time lags. The coherence is effectively the correlation of wave 1 with other altitudes and times. We calculate this coherence using the period 1 May to 15 September 2002. This period is chosen to understand the wave-1 events prior to the late-

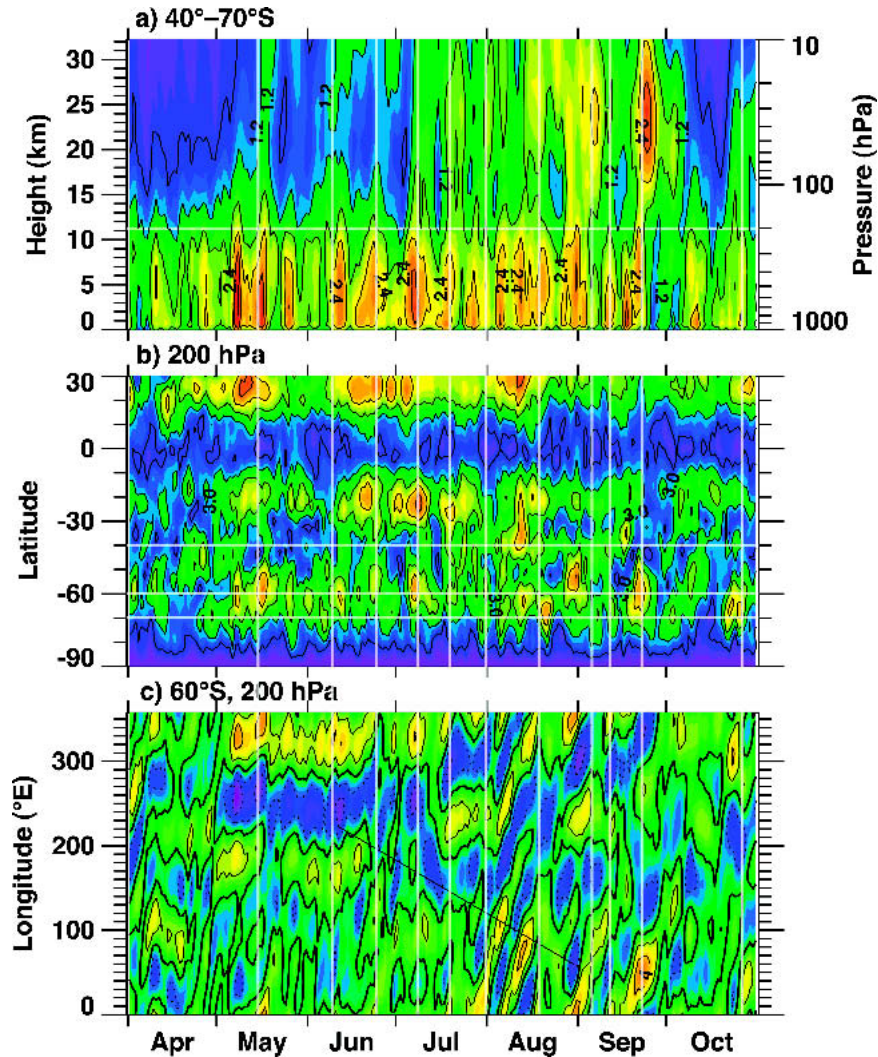


FIG. 6. Daily streamfunction, which is derived from the nondivergent components of the wind field on pressure surfaces. The streamfunction values are normalized by the radius of the earth. (a) The streamfunction wave-1-3 amplitude is averaged over 40° - 70° S. The wave amplitude is normalized by the density. The horizontal gray line shows the 200-hPa level used in (b). Color intervals are 0.2 m s^{-1} and black contour lines intervals are 0.6 m s^{-1} . (b) The streamfunction wave-1-3 amplitude at 200 hPa. The gray horizontal lines at 40° and 70° S show the range used in (a), while the horizontal gray line at 60° S shows the value used in (c). Color intervals are 0.5 m s^{-1} and black contour lines intervals are 1.5 m s^{-1} . (c) Longitude-time plot of wave-1-3 deviations from the zonal mean at 60° S and 200 hPa. Color intervals are 0.5 m s^{-1} and black contour lines intervals are 2.0 m s^{-1} . The vertical lines passing through (a)-(c) indicate the days of max eddy heat flux at 100 hPa.

September major warming. Following Randel (1987), the 95% confidence limit is on average 0.55 in the tropical troposphere and is 0.45 in the midlatitude troposphere.

There is strong wave-1 coherence between the troposphere and 100 hPa. This coherence is shifted backward by 2-3 days between 100 hPa and the surface. The peak of the coherence from 100 hPa is shifted forward in time at 10 hPa by about 2 days. This tilt of the coherence is directly related to the upward propagation of

wave-1 energy with a wave-1 group velocity of approximately 6 km day^{-1} . Plots for waves 2 and 3 show similar coherence but with faster vertical propagation (Hoskins and Karoly 1982; Randel 1987). This coherence pattern is in good agreement with the EP flux propagation shown in Fig. 5, quantitatively confirms the time lag in the wave events between the middle troposphere and middle stratosphere, and is in reasonably good agreement with theoretical estimates of the group velocity for wave 1.

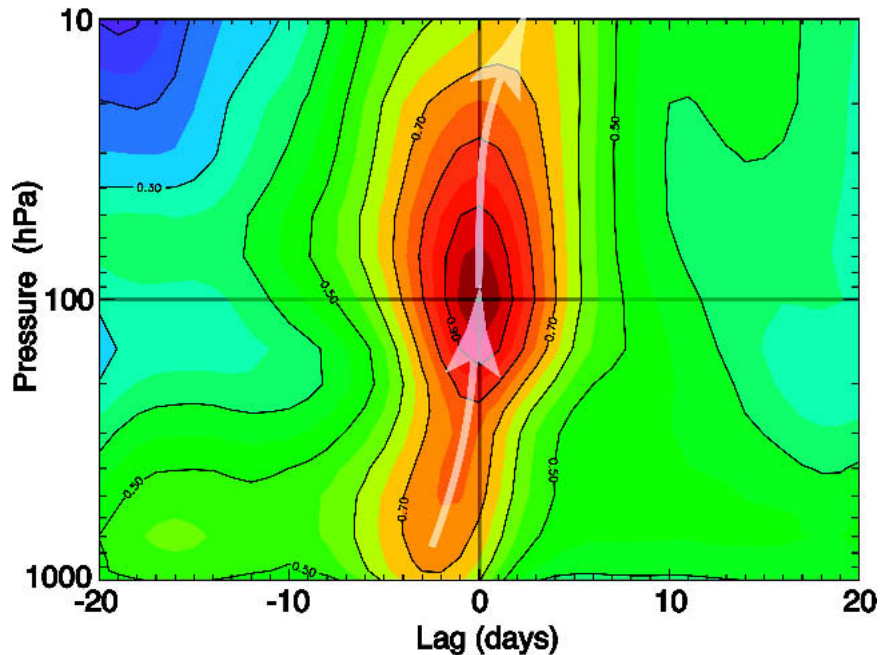


FIG. 7. The 100-hPa, 60°S wave-1 coherence of the streamfunction plotted as a function of pressure and time lag. Coherency is similar to a correlation coefficient and represents linearly related temporal variability between points. The white arrows are drawn onto the axis of the max of the coherency to illustrate the vertical propagation of wave 1. Contour intervals are 0.1.

The horizontal propagation of waves can also be observed in the streamfunction. As noted earlier, the possible association of subtropical wave 1 with the midlatitude wave 1 ought to be evident in the cross-correlation analysis. Figure 6b shows the streamfunction amplitude of waves 1–3 over the course of the season as plotted against latitude. As discussed earlier, the strong wave-1 events of 15 May, 8 July, 18 August, 22 September, and 26 October are all associated with larger than normal wave amplitudes in the 55°–70°S region. These episodes of strong wave 1 are also accompanied by strong wave events that occur in the 10°–25°S region (equatorward of the subtropical jet). However, the events in the 10°–25°S region typically occur a few days prior to the high-latitude events. Furthermore, the wave-1 events in the southern Tropics are associated with strong wave-1 events in the northern Tropics. This northern tropical wave 1 tends to also precede the southern maximum by a day or so. Hence, the wave-1 events in the southern stratosphere appear to be associated with wave events that develop in the Tropics and propagate southward.

We have investigated this association of horizontal planetary-scale wave propagation from the subtropics using the same cross-correlation analysis of the streamfunction as for Fig. 7, but using 200 hPa and 30°S as our reference point. Figure 8 shows the cross coherency for wave 1 at 30°S and 200 hPa with wave 1 at other latitudes and time lags. Again, the 95% confidence limit is approximately 0.55. There is a very strong relationship between wave 1 at 30°S and wave 1 across the Tropics

and into the NH subtropics. The exception is a node near the equator. This node results from the standing wave pattern and the 180° phase shift across the equator. The maxima in the coherency in the NH slightly precedes the SH maxima. This “tropical” coherence has a time scale of approximately 20 days. The coherency maxima at 30°S is followed approximately 4 days later by a significant coherency maxima at 60°S. Again, the 30° and 60°S coherency maxima are separated by a node that has a standing wave pattern.

We have also examined the coherence of waves 2 and 3 during the winter of 2002. Both waves 2 and 3 show distinct vertical propagation into the stratosphere but virtually no relationship to the subtropics.

Following Fig. 8, we can further trace the movement of wave 1 in the middle to lower troposphere by plotting the coherency as a function of latitude and altitude for fixed time lags. Figure 9 displays the coherence between the 200 hPa and 30°S point (denoted by a small black cross in all four panels) and all of the points on a latitude versus pressure plot for time lags of –4, 0, 2, and 4 days. As was shown with Fig. 8, all of the panels in Fig. 9 show the coherence of the 30°S wave-1 pattern across the equator and into the NH subtropics. The slightly higher maxima of the NH subtropics 4 days prior to the 30°S, 200 hPa maxima is indicated by the white × in Fig. 9a. Interestingly, this plot shows the coherence of the upper-tropospheric anticyclones in the NH and SH subtropics with cyclonic circulations in the lower troposphere. This pattern is evident in all four

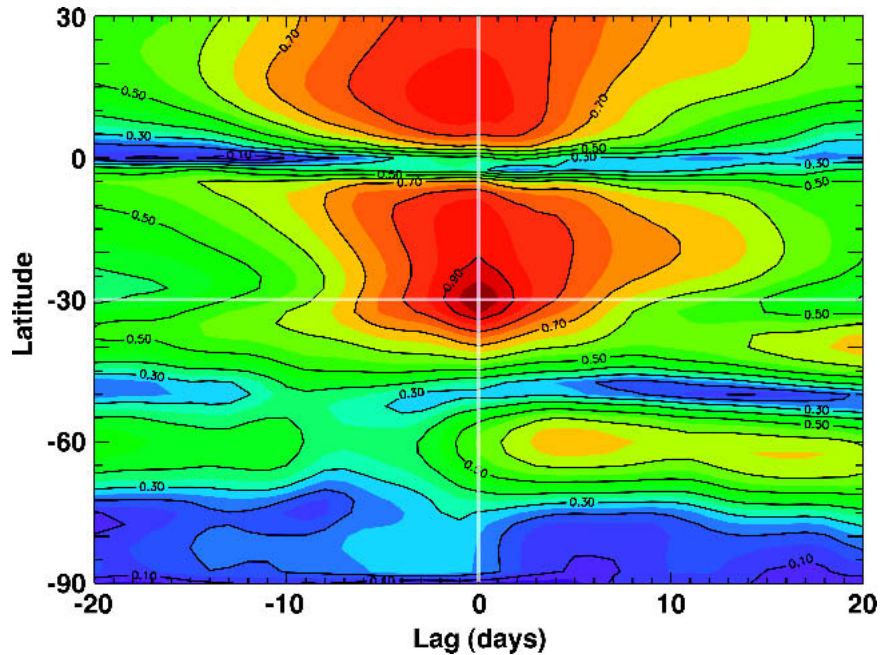


FIG. 8. The 200-hPa, 30°S wave-1 coherency of the streamfunction plotted as a function of latitude and time lag. Contour intervals are 0.1. The white lines indicate 0 lag and 30°S.

panels of Fig. 9, and forms a “quadrupole” pattern in the Tropics with a vertical node near the equator and a horizontal node at about 400 hPa.

The 30°S, 200 hPa wave-1 reference point shows a significant relationship to the midlatitude lower troposphere near 55°S, 700 hPa in the 0, +2, and +4 day lag panels (Fig. 9b,c,d). The white \times in the +2 day panel of Fig. 9c shows this coherency maxima.

The coherency maxima from 55°S and 700 hPa extend upward toward the stratosphere at 60°S in the +4 day panel of Fig. 9d, as indicated by the white \times . This intensifying coherence into the stratosphere is consistent with the vertical coherence seen in Fig. 7. The +4 day lag panel (Fig. 9d) also shows a weakening wave 1 in the Tropics.

The wave-1 coherency plots reveal a sequence of events in the winter of 2002 that begins with a strong wave 1 that spans the Tropics. This wave 1 is followed 2 days later by the development of wave 1 in the midlatitude lower troposphere (700 hPa and 55°S). The midlatitude wave 1 then takes 1–2 days to propagate into the lower stratosphere.

To understand the coherence of the SH subtropics and the SH midlatitude lower troposphere, we have examined the EP flux to determine whether waves forced in the subtropics may be propagating into the midlatitudes. First, we calculate the autocorrelation of the 100-hPa eddy heat flux against the wave-1 EP flux vectors. We determine this by regressing the 100-hPa heat flux against the components of the wave-1 EP flux vectors at all latitudes and pressures. A strong 100-hPa eddy heat flux ought to be accompanied by a strong

upward flux 1–2 days earlier from the lower troposphere, and a strong flux 1–2 days later in the middle stratosphere. Using this regression at various time lags, we estimate the effect a one standard deviation increase in 100-hPa eddy heat flux averaged over 40°–70°S has on the wave-1 EP flux. For the period 1 May to 15 September, each component of the EP flux and the zonal-mean wind is regressed against the eddy heat flux at each latitude and height. For each point in space, the value of eddy heat flux that is one standard deviation away from the average is then determined. These values are multiplied with the slope of the regression to determine the value of each EP flux component and the zonal-mean wind at each point. To determine the significance of these values, the cross-correlation between each of the EP flux components and the eddy heat flux is calculated. The 95% confidence level of the cross-correlations is calculated as in Randel (1987).

Figure 10 shows the results of various lags from –8 to +6 days. Only those vectors whose components are both significant are plotted. There is a strong southward flux between 150 and 300 hPa, 0° and 20°S that occurs prior to the peak of the 100-hPa heat flux (negative lags). There is also a strong southward flux at 850 hPa in this same subtropical latitude range.

Starting at –2 day lag, there is a strong upward and poleward component of the EP flux in the troposphere below 100 hPa at 40°–60°S. This continues through +2 day lag. Above 100 hPa, the wave pulse can be seen to rise through atmosphere and is greatly reduced by +6 day lag.

This pattern suggests that the midlatitude lower-

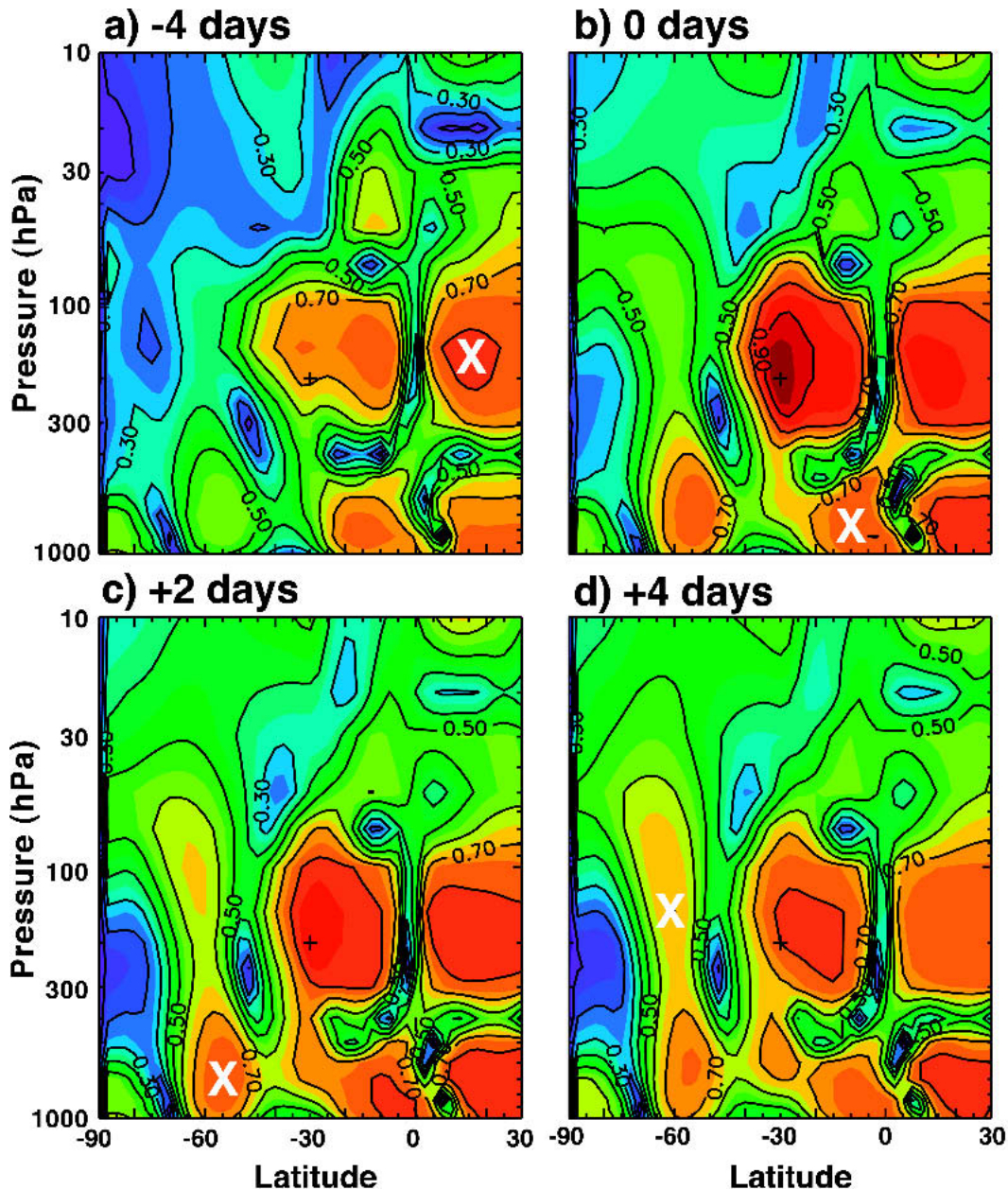


FIG. 9. Contour plots of the 200-hPa, 30°S wave-1 coherency plotted as a function of altitude and latitude for phase lags of (a) -4, (b) 0, (c) +2, and (d) +4 days. The white \times 's are reference points for discussion in the text. The black crosses indicate the 200-hPa, 30°S point. Contour intervals are 0.1.

tropospheric wave-1 development seen in Figs. 9b–d results from a southward wave-1 propagation from the subtropics that is associated with the upper-tropospheric wave-1 pattern. As wave 1 amplifies in the mid-latitude lower troposphere, it bifurcates with one branch moving poleward and upward into the stratosphere and the second branch moving upward and equatorward into the tropospheric subtropical jet. This bifurcation is seen in the midlatitude middle to lower troposphere of the 0-day lag panel.

Because of the strong coherence between wave 1 at 200 hPa and wave 1 at 700 hPa 2–3 days earlier, we have examined the interannual behavior of the streamfunction at 700 hPa in the midlatitudes and at 200 hPa in the subtropics. Figure 11a displays the average wave-1 amplitude between 10° and 30°S at 200 hPa for each year from 1979 to 2002 for a 1 May–15 September average. In this figure, 2002 stands out as the record value. As noted above, the wave-1 amplitude at 700 hPa is related to the tropical wave-1 amplitude with about a 4-day lag.

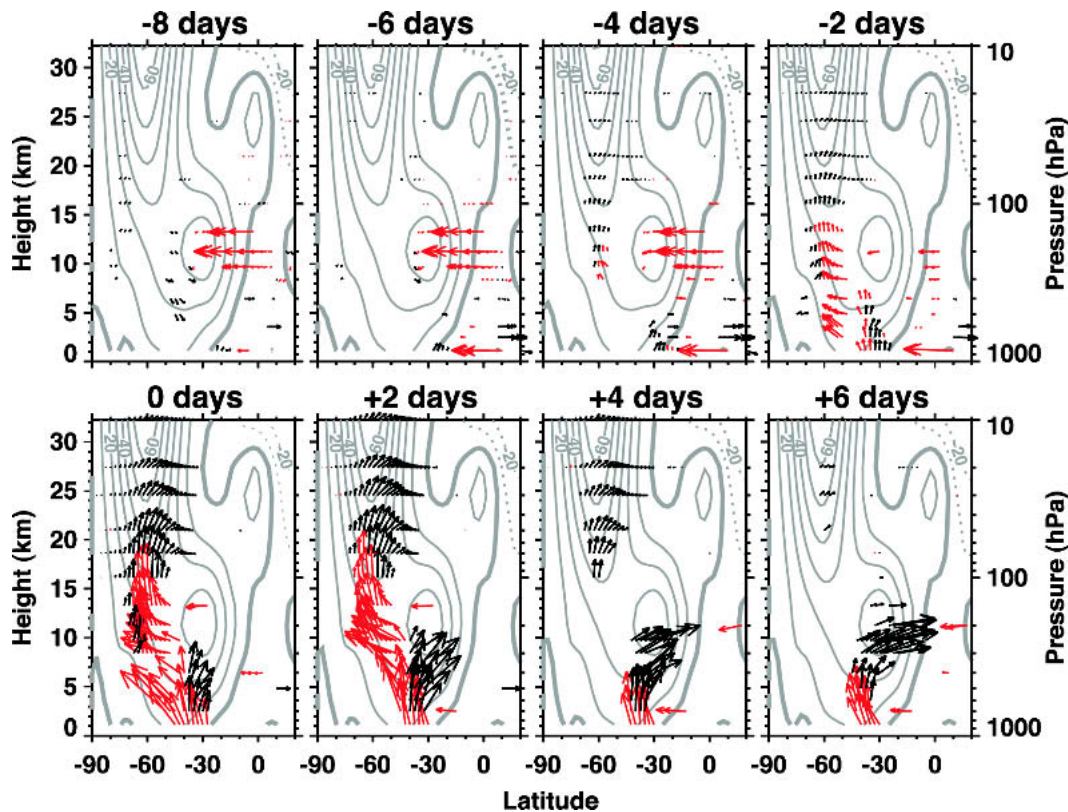


FIG. 10. Wave-1 EP flux vectors calculated from a one-standard-deviation increase in 100-hPa eddy heat flux for various time lags (see text for explanation). Data are from 1 May to 15 Sep. Only significant EP flux vectors have been plotted. Black arrows point equatorward and red arrows point poleward. The gray contours represent the zonal-mean zonal wind field resulting from the same one-standard-deviation increase in eddy heat flux. Contour intervals are 10 m s^{-1} .

Figure 11b displays the average wave-1 amplitude between 50° and 70°S at 700 hPa for each year from 1979 to 2002 for the same 1 May–15 September average (no time lag). Again, the wave-1 amplitude in the southern Tropics is a maximum. The two time series have a 0.51 correlation, which for 24 years that are independent is significantly different from zero at the 99% confidence level using a two-sided Student's t test. However, this correlation only explains about 26% of the variance in the wave-1 700-hPa variance.

4. Discussion

The SH stratosphere was extremely disturbed during the winter of 2002. The culmination of this disturbed stratosphere was the major warming of 22 September. There are two hypotheses to explain this increase in stratospheric wave activity: 1) excessive tropospheric wave forcing in 2002 propagating upward into the stratosphere and 2) an anomalous mean flow that allowed moderate tropospheric waves to more easily propagate into the stratosphere.

The tropospheric wave forcing was higher than aver-

age during the 2002 winter. For April–September, the 200-hPa heat flux for waves 1–3 between 40° and 70°S was 50% stronger than climatology and substantially stronger than any previous year. If we exclude September from this average, then the heat flux was still about 40% stronger than climatology, but comparable to both 1992 and 1995. While it was higher than average, wave forcing was not at record levels near the tropopause. However, as was shown in Fig. 11b, wave 1 was anomalously larger in the lower troposphere. This higher than normal wave 1 is associated with higher than normal wave 1 in the Tropics. Both waves 2 and 3 were also higher than normal in 2002 but did not show any relationship to tropical wave forcing.

From the coherence in Fig. 9, wave 1 at 200 hPa and 30°S is strongly correlated with the northern subtropical waves. This suggests that coherent tropical wave-1 fluctuations across the Tropics result in propagation of subtropical wave energy southward in the lower troposphere into the southern midlatitude lower troposphere, reinforcing the wave 1 in the lower troposphere, which then propagates upward into the stratosphere.

Karoly et al. (1989) have analyzed height field data to diagnose 3D wave propagation in the SH. In contrast to

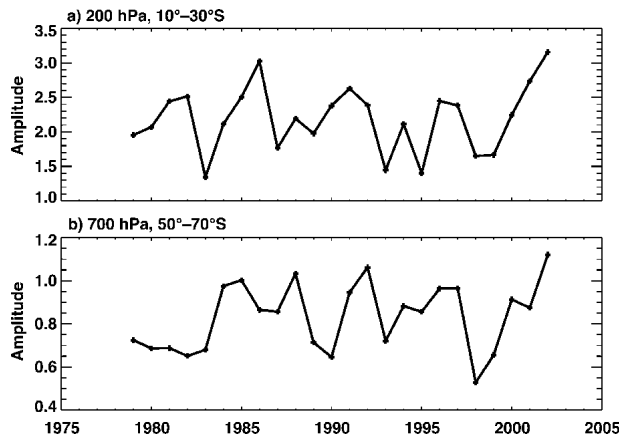


FIG. 11. Amplitude of the wave-1 streamfunction for 1979–2002 averaged over 1 May–15 Sep for each year. (a) The streamfunction at 200 hPa and averaged for 10° – 30° S. (b) The streamfunction at 700 hPa and averaged for 50° – 70° S. The streamfunction is derived from the nondivergent part of the meridional and zonal winds on pressure surfaces.

NH topographically forced height anomalies, they found a poor association between the SH stationary height field anomalies and the 3D wave flux. They suggested that the forcing of the larger-scale waves was associated with the midlatitude jet and eddy forcings rather than topography or large-scale thermal forcing. The EP flux diagrams in Fig. 10 show some wave-1 propagation near the surface into the midlatitudes, but the correlation of subtropical EP flux near the surface with the vertical EP flux into the stratosphere is small. These results show that, in spite of the excellent coherence between the lower stratosphere and the Tropics, there is not a straightforward relationship between the Tropics and the midlatitudes.

The weaker stratospheric winds and warmer temperatures seen in 2002 are clearly consistent with the greater wave forcing observed in the stratosphere, as has been shown in the modeling study of Taguchi and Yoden (2002). These waves are forced in the troposphere and propagate into the stratosphere. However, the strong forcing of these large-scale waves in the troposphere is quantitatively difficult to explain. Large wave forcing from the SH troposphere is consistent with the modeled dynamic forcing discussed in Scinocca and Haynes (1998). In their model, stratospheric wave activity was forced by nonlinear wave–wave interaction of tropospheric baroclinic waves. This wave–wave interaction was characterized by waves with relatively slow phase velocities embedded in wave packets with large group velocities. However, they noted that it was not always possible to associate forcing of waves with bursts of upward EP flux. The upper tropospheric eddies do not show clear evidence of excessively strong wave packets.

The wave propagation is controlled by the index of refraction, which is proportional to the meridional po-

tential vorticity (PV) gradient and inversely proportional to the zonal-mean zonal wind minus the wave's phase speed (Dickinson 1968). As was noted in Fig. 2b, the zero-wind line was 6° – 10° closer to the pole in 2002. At 10 hPa, the 20 m s^{-1} zonal-mean zonal wind is usually found at 36.4° S. In 2002, the 20 m s^{-1} zonal-mean zonal wind was found at 43.6° S. During August 2002 (preceding the major warming), the polar-night jet was the weakest yet observed, and the equatorial flank of the jet was located at the most southerly latitude since 1988. This implies that slow-moving planetary waves would encounter a critical line at a more southerly latitude than was normally found in past years. This anomalous jet structure was also found in earlier months of 2002. For example, in April (prior to any wave events noted herein), the subtropical zonal winds in the upper stratosphere were anomalously easterly, and the jet was a few degrees closer to the pole than normal. The structure of the zonal-mean zonal wind during 2002 was anomalous, suggesting that wave propagation was more focused into the polar region during 2002, prior to the major warming.

The impact of tropical and extratropical winds on stratospheric variability has been shown by Holton and Tan (1982). They showed that the QBO impacted wave propagation in the NH stratosphere and hence the interannual variability of the polar vortex. Gray et al. (2001a) extended this work to show that upper-stratospheric winds dramatically impacted NH polar vortex variability, while Gray et al. (2001b) utilized a model to show that middle- to upper-stratospheric equatorial winds were necessary to explain the Holton–Tan relationship. Scott and Haynes (1998) have also used a model to demonstrate that disturbed winters are accompanied by late-fall to early-winter easterlies in the subtropics. Indeed, such easterlies were observed in 2002 in the Tropics in association with a westerly QBO at 30 hPa. In fact, temperatures near the vortex edge in early September are highly anticorrelated with tropical winds in the upper stratosphere.

The index of refraction at the tropopause was slightly more conducive to waves propagating into the stratosphere. Chen and Robinson (1992) suggested that the refractive index at the tropopause acted as a valve for the propagation of planetary waves. Figure 12 is a plot of the 45° – 75° S 100-hPa heat flux plotted against the quasigeostrophic PV meridional gradient as a function of year, averaged between 400 and 100 hPa, 40° and 60° S. The quantities are time averaged from 1 May to 15 September for each year. The correlation between the heat flux and PV gradient is 0.75. If we perform a multiple regression of the 500-hPa heat flux (tropospheric wave forcing) and PV gradient (index of refraction) against the 100-hPa heat flux, the correlation increases to 0.9. This is consistent with the hypothesis that the wave energy that has entered the stratosphere is directly related to the tropospheric forcing and the

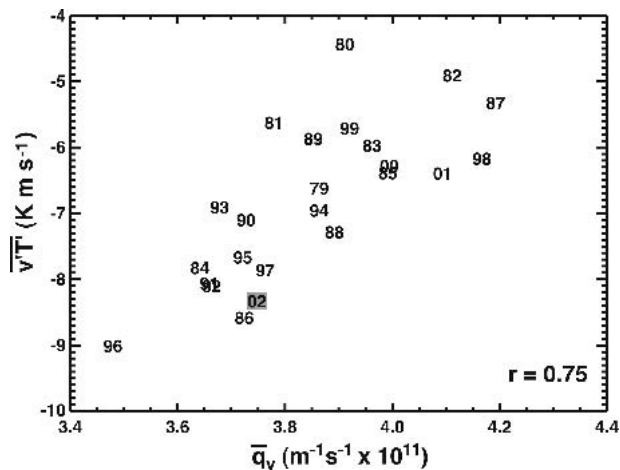


FIG. 12. The 100-hPa eddy heat flux $\overline{v'T'}$ vs the meridional gradient of the quasigeostrophic potential vorticity ($\overline{q_y}$) averaged over 1 May–15 Sep for each year. The eddy heat flux is averaged for 45° – 75° S, while $\overline{q_y}$ is averaged for 40° – 60° S and 100–400 hPa. The index of refraction is proportional to $\overline{q_y}$. The correlation is 0.55. Each year is indicated by the last two digits.

valving near the tropopause controlled by the index of refraction.

The subtropical jet stream was also anomalous during the 2002 SH winter. This jet was both weaker than normal and shifted poleward by 1.8° during the winter. This jet shift would also shift large values of the index of refraction poleward, resulting in wave propagation that was oriented more upward than equatorward, as would occur in a normal year.

5. Summary and conclusions

The 2002 SH winter had perhaps the most interesting stratospheric conditions yet observed since stratospheric observations first began in the 1940s. This winter had the only major stratospheric warming ever observed in the SH. While such major warmings are relatively common in the NH, the typical warming of the SH only occurs in the final warming during October–November. The warmer temperatures and stronger wave dynamics significantly impacted the Antarctic ozone hole.

The 2002 hole was the least severe since 1988. The 2002 wave events dramatically impacted the Antarctic ozone hole (Stolarski et al. 2005). Using Total Ozone Mapping Spectrometer ozone measurements, the size of the hole was already small during the period preceding the major warming. This smaller size is consistent with the warmer temperatures at the vortex edge. The major warming then split the Antarctic ozone. The ozone hole had an early disappearance in response to the final wave event on 26 October.

The mean temperature of the polar lower stratosphere was much warmer than normal during the win-

ter of 2002. The temperature of the Antarctic stratosphere was directly related to the wave forcing events observed over the course of the winter. This 2002 strong eddy forcing of the SH stratosphere is uncommon, but the resulting high temperatures were generally consistent with the magnitude and timing of the forcing. Hence, the higher-than-normal polar temperatures did not result from any direct radiative forcing mechanism.

The SH stratospheric wind fields were also highly anomalous during the winter of 2002. This was especially true following the major warming of 22 September. However, it is also clear that the winds were abnormal as far back as April. The anomalous easterlies in the middle to upper stratosphere intensified over the course of the winter with the jet becoming progressively weaker and moving closer to the pole. The wave events up through early September preconditioned the zonal-mean zonal wind field and the index of refraction to allow the major warming of 22 September.

The stronger than normal wave 1 in the stratosphere is associated with strong forcing of wave 1 in the subtropics of the NH and SH. First, the stratospheric wave 1 observed during 2002 is statistically related to the lower troposphere with a 2-day lag, and this wave 1 in the lower troposphere is highly correlated with the tropical wave 1. Second, EP flux diagrams show wave propagation from the subtropics, followed by upward propagation into the stratosphere, albeit, this correlation is weak. Third, the 2002 winter average wave-1 amplitudes in both the midlatitude lower troposphere and tropical upper troposphere were the largest values observed in the 24-yr record. While the EP flux and correlation diagnostics provide a strong case for a tropical wave-1 forcing, the magnitude of the EP flux in the stratosphere is excessive in comparison to the tropospheric forcing.

The winter dynamics of 2002 is directly responsible for the unusual ozone hole, and the unusual dynamics results from higher than average wave forcing from the troposphere. In particular, we find that the larger than normal propagation of planetary-scale waves into the stratosphere was caused by two main factors: 1) stronger than normal levels of planetary wave 1 in the southern midlatitude lower troposphere and 2) a propagation state that was conducive to upward propagation of waves (i.e., a lower than normal index of refraction at the tropopause that allowed more wave penetration into the stratosphere, and tropical upper-stratospheric easterlies).

To briefly summarize, planetary-scale wave events in the midlatitude troposphere (near 700 hPa, 55° S) occurred episodically on a 1–2 week time scale over the course of the SH winter. Because the zonal-mean flow at the tropopause and in the tropical upper stratosphere was conducive to wave propagation, the planetary-scale waves in the lower troposphere were efficiently refracted upward into the stratosphere. Each wave event warmed the polar lower stratosphere and weakened the

jet stream. By the middle of September, the cumulative effect of the wave events had preconditioned the stratospheric zonal-mean zonal wind pattern to allow the occurrence of a major warming. A large event on 22 September then resulted in a major warming of the stratosphere. This warming was strong enough to warm temperatures beyond the formation point for polar stratospheric clouds, thereby stopping ozone loss. The wave events in the midlatitude troposphere are statistically related to the wave events in the subtropical troposphere. These subtropical wave events took 2–4 days to propagate from the subtropics into the lower troposphere near 55°S. The theoretical connection of these subtropical waves to the midlatitude troposphere is not understood.

Acknowledgments. We wish to thank Drs. Darryl Waugh, Warrick Norton, Mark Schoeberl, Lorenzo Polvani, Lesley Gray, and Matthew Hitchman for helpful discussions. This work was supported under a NASA grant from the Atmospheric Chemistry, Modeling, and Analysis Program.

REFERENCES

- Andrews, D. G., J. R. Holton, and C. B. Leovy, 1987: *Middle Atmosphere Dynamics*. Academic Press, 489 pp.
- Chen, P., and W. A. Robinson, 1992: Propagation of planetary waves between the troposphere and stratosphere. *J. Atmos. Sci.*, **49**, 2533–2545.
- Court, A., 1942: Tropopause disappearance during the Antarctic winter. *Bull. Amer. Meteor. Soc.*, **23**, 220–238.
- Dickinson, R. E., 1968: Planetary Rossby waves propagating vertically through weak westerly wind wave guides. *J. Atmos. Sci.*, **25**, 984–1002.
- Gray, L. J., E. F. Drysdale, T. J. Dunkerton, and B. N. Lawrence, 2001a: Model studies of the interannual variability of the Northern Hemisphere stratospheric winter circulation: The role of the quasi-biennial oscillation. *Quart. J. Roy. Meteor. Soc.*, **127**, 1413–1432.
- , S. J. Phipps, T. J. Dunkerton, M. P. Baldwin, E. F. Drysdale, and M. R. Allen, 2001b: A data study of the influence of the equatorial upper stratosphere on Northern Hemisphere stratospheric sudden warmings. *Quart. J. Roy. Meteor. Soc.*, **127**, 1985–2003.
- Hartmann, D. L., C. R. Mechoso, and K. Yamazaki, 1984: Observations of wave–mean flow interaction in the Southern Hemisphere. *J. Atmos. Sci.*, **41**, 351–362.
- Holton, J. R., and H. C. Tan, 1982: The quasi-biennial oscillation in the Northern Hemisphere lower stratosphere. *J. Meteor. Soc. Japan*, **60**, 140–148.
- Hoppel, K., R. Bavailacqua, D. Allen, G. Nedoluha, and C. Randall, 2003: POAM III observations of the anomalous 2002 Antarctic ozone hole. *Geophys. Res. Lett.*, **30**, 1394, doi:10.1029/2003GL016899.
- Hoskins, B. J., and D. J. Karoly, 1981: The steady linear response of a spherical atmosphere to thermal and orographic forcing. *J. Atmos. Sci.*, **38**, 1179–1196.
- Kanamitsu, M., R. E. Kistler, and R. W. Reynolds, 1997: NCEP/NCAR reanalysis and the use of satellite data. *Adv. Space Res.*, **19**, 481–489.
- Karoly, D. J., R. A. Plumb, and M. Ting, 1989: Examples of the horizontal propagation of quasi-stationary waves. *J. Atmos. Sci.*, **46**, 2802–2811.
- Marshall, G. J., 2002: Trends in Antarctic geopotential height and temperature: A comparison between radiosonde and NCEP–NCAR reanalysis data. *J. Climate*, **15**, 659–674.
- Mo, K. C., X. L. Wang, R. Kistler, M. Kanamitsu, and E. Kalnay, 1995: Impact of satellite data on the CDAS reanalysis system. *Mon. Wea. Rev.*, **123**, 124–139.
- Montzka, S. A., J. H. Butler, B. D. Hall, D. J. Mondeel, and J. W. Elkins, 2003: A decline in tropospheric organic bromine. *Geophys. Res. Lett.*, **30**, 1826, doi:10.1029/2003GL017745.
- Newman, P. A., and E. R. Nash, 2000: Quantifying the wave driving of the stratosphere. *J. Geophys. Res.*, **105**, 12 485–12 497.
- , —, and J. E. Rosenfield, 2001: What controls the temperature of the Arctic stratosphere during the spring? *J. Geophys. Res.*, **106**, 19 999–20 010.
- Randel, W. J., 1987: A study of planetary waves in the southern winter troposphere and stratosphere. Part I: Wave structure and vertical propagation. *J. Atmos. Sci.*, **44**, 917–935.
- , 1992: Global atmospheric circulation statistics, 1000–01 mb. NCAR Tech. Note NCAR/TN-366+STR, 256 pp.
- , F. Wu, and R. Stolarski, 2002: Changes in column ozone correlated with the stratospheric EP flux. *J. Meteor. Soc. Japan*, **80**, 849–862.
- Rex, M., and Coauthors, 2002: Chemical depletion of Arctic ozone in winter 1999/2000. *J. Geophys. Res.*, **107**, 8276, doi:10.1029/2001JD000533.
- Santer, B. D., J. J. Hnilo, T. M. L. Wigley, J. S. Boyle, C. Doutriaux, M. Fiorino, D. E. Parker, and K. E. Taylor, 1999: Uncertainties in observationally based estimates of temperature change in the free atmosphere. *J. Geophys. Res.*, **104**, 6305–6333.
- Scinocca, J. F., and P. H. Haynes, 1998: Dynamical forcing of stratospheric planetary waves by tropospheric baroclinic eddies. *J. Atmos. Sci.*, **55**, 2361–2392.
- Scott, R. K., and P. H. Haynes, 1998: Internal interannual variability of the extratropical stratospheric circulation: The low-latitude flywheel. *Quart. J. Roy. Meteor. Soc.*, **124**, 2149–2173.
- Shiotani, M., and J. C. Gille, 1987: Dynamic factors affecting ozone mixing ratios in the Antarctic lower stratosphere. *J. Geophys. Res.*, **92**, 9811–9824.
- Stolarski, R. S., R. D. McPeters, and P. A. Newman, 2005: The ozone hole of 2002 as measured by TOMS. *J. Atmos. Sci.*, **62**, 716–720.
- Taguchi, M., and S. Yoden, 2002: Internal interannual variability of the troposphere–stratosphere coupled system in a simple global circulation model. Part I: Parameter sweep experiment. *J. Atmos. Sci.*, **59**, 3021–3036.
- WMO, 1995: Scientific assessment of ozone depletion: 1994. Rep. 37, Global Ozone Research and Monitoring Project, 473 pp.